Inorg. Chem. **2007**, *46*, 7971–7981

Synthesis and Electrochemistry of New Rh-Centered and Conjuncto Rhodium Carbonyl Clusters. X-ray Structure of $[NEt_4]_3[Rh_{15}(CO)_{27}]$, $[NEt_4]_3[Rh_{15}(CO)_{25}(MeCN)_2]\cdot 2MeCN$, and $[NEt_4]_3[Rh_{17}(CO)_{37}]$

Davide Collini,[†] Fabrizia Fabrizi De Biani,[‡] Serena Fedi,[‡] Cristina Femoni,[†] Francesco Kaswalder,[†] Maria Carmela Iapalucci,[†] Giuliano Longoni,*[,†] Cristina Tiozzo,[†] Stefano Zacchini,[†] and Piero Zanello[‡]

Dipartimento di Chimica Fisica ed Inorganica, Università di Bologna, viale Risorgimento 4, 40136 Bologna, Italy, and Dipartimento di Chimica, Università di Siena, via A. Moro, 53100 Siena, Italy

Received December 12, 2006

A reinvestigation of the redox chemistry of $[Rh_7(CO)_{16}]^{3-}$ resulted in the finding of new alternative syntheses for a series of previously reported Rh-centered carbonyl clusters, i.e., $[H_{4-n}Rh_{14}(CO)_{25}]^{n-}$ ($n = 3$ and 4) and $[Rh_{17}(CO)_{30}]^{3-}$, as well as new species such as a different isomer of $[Rh_{15}(CO)_{27}]^{3-}$, the carbonyl-substituted $[Rh_{15}(CO)_{25}(MeCN)_2]^{3-}$, and the conjuncto $[Rh_{17}(CO)_{37}]^{3-}$ clusters. All of the above clusters are suggested to derive from oxidation of $[Rh_7(CO)_{16}]^{3-}$ with H^+, arising from dissociation either of $[M(H_2O)_n]^{2+}$ aquo complexes or nonoxidizing acids. The nature of the previously reported species has been confirmed by IR, electrospray ionization mass spectrometry, and complete X-ray diffraction studies. Only the molecular structures of the new clusters are reported in some details. The ready conversion of $[Rh_7(CO)_{16}]^{3-}$ in $[HRh_{14}(CO)_{25}]^{3-}$ upon oxidation has been confirmed by electrochemical techniques. In addition, electrochemical studies point out that the close-packed $[H_3Rh_{13}(CO)_{24}]^{2-}$ dianion undergoes a reversible monoelectronic reduction followed by an irreversible reduction. The irreversibility of the second reduction is probably a consequence of H_2 elimination from a purported $[H_3Rh_{13}(CO)_{24}]^{4-}$ species. Conversely, the body-centered-cubic $[HRh_{14}(CO)_{25}]^{3-}$ and $[Rh_{15}(CO)_{27}]^{3-}$ trianions display several well-defined redox changes with features of electrochemical reversibility, even at low scan rate. The major conclusion of this work is that mild experimental conditions and a tailored oxidizing reagent may enable more selective conversion of $[Rh_7(CO)_{16}]^{3-}$ into a higher-nuclearity rhodium carbonyl cluster. It is also shown that isonuclear Rh clusters may display isomeric metal frameworks [i.e., $[Rh_{15}(CO)_{27}]^{3-}$], as well as almost identical metal frames stabilized by a different number of carbonyl groups [i.e., $[Rh_{15}(CO)_{27}]^{3-}$ and $[Rh_{15}(CO)_{30}]^{3-}$]. Other isonuclear Rh clusters stabilized by a different number of CO ligands more expectedly exhibit completely different metal geometries [i.e., $[Rh_{17}(CO)_{30}]^{3-}$ and $[Rh_{17}(CO)_{37}]^{3-}$]. The first pair of isonuclear and isoskeletal clusters is particularly astonishing in that $[Rh_{15}(CO)_{30}]^{3-}$ features six valence electrons more than $[Rh_{15}(CO)_{27}]^{3-}$. Finally, the electrochemical studies seem to suggest that interstitial Rh atoms are less effective than Ni and Pt interstitial atoms in promoting redox properties and inducing molecular capacitor behavior in carbonyl clusters.

Introduction

Several metal carbonyl clusters containing interstitial Ni, Pt, or Ag atoms may be considered as molecular nanocapacitors. Indeed, they display reversible electron-sink behavior, are sometimes multivalent (being a given cluster stable with a different number of charges), and trespass from the bottom in the field of nanosized materials.[1,2] These features candidate their possible application in molecular nanolithography and electronics.[3−5] The above statements are

* To whom correspondence should be addressed. E-mail: longoni@ms.fci.unibo.it. Phone: 00-051-2093711. Fax: 00-051-2093690.
[†] Università di Bologna.
[‡] Università di Siena.

(1) Collini, D.; Femoni, C.; Iapalucci, M. C.; Longoni, G.; Zanello, P. *Perspectives in Organometallic Chemistry*; Screttas, C. G., Steele, B. R., Eds.; RSC Books: Cambridge, U.K., 2003; Vol. 287, pp 183−195.
(2) Femoni, C.; Iapalucci, M. C.; Kaswalder, F.; Longoni, G.; Zacchini, S. *Coord. Chem. Rev.* **2006**, *250*, 1580−1604.

10.1021/ic0623718 CCC: $37.00
Published on Web 08/17/2007

supported by the behavior of species such as $[Ni_{13}Sb_2(CO)_{24}]^{n-}$ ($n = 2-4$),[6] $[Ni_{11}E_2(CO)_{18}]^{n-}$ (E = Sb and Bi; $n = 2-4$),[7,8] $[Ni_5Rh_9(CO)_{25}]^{n-}$ ($n = 2$ and 3),[9] $[Ni_{38}Pt_6(CO)_{48}]^{n-}$ ($n = 5-10$),[10] $[Pt_{19}(CO)_{22}]^{n-}$ ($n = 0-6$),[11] $[Pt_{24}(CO)_{30}]^{n-}$ ($n = 0-6$),[12,13] and $[Ag_{13}Fe_8(CO)_{32}]^{n-}$ ($n = 3-5$).[14] For a given geometry, the electrochemical behavior is greatly affected by changes in the metallic composition of the cluster framework [e.g., $[Ni_{38}Pt_6(CO)_{48}]^{6-}$ vs $[Ni_{35}Pt_9(CO)_{48}]^{6-}$][10,15] and substitution with H atoms of one or more negative charges [e.g., $[Ni_{38}Pt_6(CO)_{48}]^{6-}$ vs $[H_{6-n}Ni_{38}Pt_6(CO)_{48}]^{n-}$ ($n = 4$ and 5)].[10] This gives the additional opportunity to modulate their electronic features and tune the redox potentials of the cluster capacitor. Molecular capacities of 0.25−0.75 aF,[2] comparable to those of "monodispersed" Au−thiol nanoparticles,[16−19] are observed for cluster cores in the 13−44 range of nuclearity.[10]

The only other elements giving carbonyl cluster compounds containing interstitial metal atoms are Co (e.g., $[Co_{11}Te_7(CO)_{10}]^{-}$)[20] and Rh. The chemistry of rhodium carbonyl clusters has been widely investigated in the past by Chini and Martinengo and researchers of Union Carbide. Two slightly different synthetic approaches were adopted. The first approach consisted of the mild pyrolysis of sodium salts of a preformed rhodium carbonyl cluster (e.g., $[Rh_{12}(CO)_{30}]^{2-}$), followed by separation of the resulting mixture by differential solubility in water of the alkali salts of the miscellaneous cluster anions. The Union Carbide approach consisted of the carbonylation under pressure and high temperature of $Rh(CO)_2(acac)$ in the presence of alkaline reagents. A wide series of high-nuclearity rhodium carbonyl clusters, among which are $[H_{5-n}Rh_{13}(CO)_{24}]^{n-}$ ($n = 2-4$),[21−24] $[H_{4-n}Rh_{14}(CO)_{25}]^{n-}$ ($n = 3$ and 4),[24−28] $[Rh_{14}(CO)_{26}]^{2-}$,[24,29] $[Rh_{15}(CO)_{27}]^{3-}$,[24,25] $[Rh_{15}(CO)_{30}]^{3-}$,[30] $[Rh_{17}(CO)_{30}]^{3-}$,[31] $[Rh_{22}(CO)_{37}]^{4-}$,[32] and $[H_xRh_{22}(CO)_{35}]^{4-/5-}$,[33] have been isolated and characterized. To our knowledge, the electrochemistry of the above rhodium carbonyl clusters has not attracted previous attention. Only scattered reports on the redox behavior of heterometallic and carbonyl-substituted rhodium clusters are available.[11,34]

Our interest in rhodium cluster chemistry was fueled by the serendipitous discovery of the selective synthesis of a $[H_{4-n}Rh_{14}(CO)_{25}]^{n-}$ ($n = 3$ and 4) cluster during the investigation of the condensation of $[Rh_7(CO)_{16}]^{3-}$ with $NiCl_2 \cdot 6H_2O$ as a possible potential synthesis of $[NiRh_{14}(CO)_{28}]^{4-}$.[35] The unexpected result prompted a more detailed study of the above and related reactions with other M^{II} and M^{III} aqueous ions (M = Zn, Cd, Sn, and In). These investigations led to new syntheses of some already reported Rh clusters and isolation of several new homo- and heterometallic rhodium carbonyl clusters. We report here the results regarding the homometallic rhodium carbonyl clusters and, in particular, syntheses in mild conditions of $[H_{4-n}Rh_{14}(CO)_{25}]^{n-}$ ($n = 3$ and 4), $[Rh_{15}(CO)_{27}]^{3-}$, $[Rh_{15}(CO)_{25}(MeCN)_2]^{3-}$, $[Rh_{17}(CO)_{30}]^{3-}$, and $[Rh_{17}(CO)_{37}]^{3-}$. The structural characterization of the new Rh-centered $[Rh_{15}(CO)_{27-n}(MeCN)_n]^{3-}$ ($n = 0$ and 2) and the conjuncto $[Rh_{17}(CO)_{37}]^{3-}$ cluster is also reported. The formation of heterometallic clusters was only observed when using $SnCl_2 \cdot 2H_2O$ as the oxidizing agent. The resulting Rh−Sn clusters will be reported elsewhere. The redox properties of the Rh-centered carbonyl clusters $[H_3Rh_{13}(CO)_{24}]^{2-}$, $[HRh_{14}(CO)_{25}]^{3-}$, and $[Rh_{15}(CO)_{27}]^{3-}$, as well as those of the $[Rh_7(CO)_{16}]^{3-}$ starting material, have been investigated in order to test their molecular capacitor behavior.

(3) Carroll, R. L.; Gorman, C. B. *Angew. Chem., Int. Ed.* **2002**, *41*, 4378−4400.
(4) Schmid, G.; Simon, U. *Chem. Commun.* **2005**, 697−710.
(5) Wouters, D.; Schubert, U. S. *Angew. Chem., Int. Ed.* **2004**, *43*, 2480−2495.
(6) Albano, V. G.; Demartin, F.; Iapalucci, M. C.; Laschi, F.; Longoni, G.; Sironi, A.; Zanello, P. *J. Chem. Soc., Dalton Trans.* **1991**, 7−747.
(7) Albano, V. G.; Demartin, F.; Femoni, C.; Iapalucci, M. C.; Longoni, G.; Monari, M.; Zanello, P. *J. Organomet. Chem.* **2000**, *593−594*, 325−334.
(8) Albano, V. G.; Demartin, F.; Iapalucci, M. C.; Longoni, G.; Monari, M.; Zanello, P. *J. Chem. Soc., Dalton Trans.* **1992**, 497−502.
(9) Collini, D.; Femoni, C.; Iapalucci, M. C.; Longoni, G.; Svensson, P. H.; Zanello, P. *Angew. Chem., Int. Ed.* **2002**, *41*, 3685−3688.
(10) Fabrizi de Biani, F.; Femoni, C.; Iapalucci, M. C.; Longoni, G.; Zanello, P.; Cerotti, A. *Inorg. Chem.* **1999**, *38*, 3721−3724.
(11) Zanello, P. In *Stereochemistry of Organometallic and Inorganic Compounds*; Zanello, P., Ed.; Elsevier: Amsterdam, The Netherlands, 1994; Vol. 5, pp 163−408.
(12) Lewis, G. J.; Roth, J. D.; Montag, R. A.; Safford, L. K.; Gao, X.; Chang, S.-C.; Dahl, L. F.; Weaver, M. J. *J. Am. Chem. Soc.* **1990**, *112*, 2831−2832.
(13) Roth, J. D.; Lewis, G. J.; Safford, L. K.; Jiang, X.; Dahl, L. F.; Weaver, M. J. *J. Am. Chem. Soc.* **1992**, *114*, 6159−6169.
(14) Albano, V. G.; Calderoni, F.; Iapalucci, M. C.; Longoni, G.; Monari, M.; Zanello, P. *J. Cluster Sci.* **1995**, *6*, 107−123.
(15) Femoni, C.; Iapalucci, M. C.; Longoni, G.; Svensson, P. H.; Zanello, P.; Fabrizi De Biani, F. *Chem.−Eur. J.* **2004**, *10*, 2318−2326.
(16) Ingram, R. S.; Hostetler, M. J.; Murray, R. W.; Schaaff, T. G.; Khoury, J. T.; Whetten, R. L.; Bigioni, T. P.; Guthrie, D. K.; First, P. N. *J. Am. Chem. Soc.* **1997**, *119*, 9279−9280.
(17) Hicks, J. F.; Templeton, A. C.; Chen, S.; Sheran, K. M.; Jasti, R.; Murray, R. W.; Debord, J.; Schaaff, T. G.; Whetten, R. L. *Anal. Chem.* **1999**, *71*, 3703−3711.
(18) Miles, D. T.; Murray, R. W. *Anal. Chem.* **2003**, *75*, 1251−1257.
(19) Quinn, B. M.; Liljeroth, P.; Ruiz, V.; Laaksonen, T.; Kontturi, K. *J. Am. Chem. Soc.* **2003**, *125*, 6644−6645.
(20) Brunner, H.; Cattey, H.; Meier, W.; Mugnier, Y.; Stuckl, A. C.; Wachter, J.; Wanninger, R.; Zabel, M. *Chem.−Eur. J.* **2003**, *9*, 3796−3802.
(21) Albano, V. G.; Ceriotti, A.; Chini, P.; Ciani, G.; Martinengo, S.; Anker, W. M. *J. Chem. Soc., Chem. Commun.* **1975**, 859−860.
(22) Albano, V. G.; Ciani, G.; Martinengo, S.; Sironi, A. *J. Chem. Soc., Dalton Trans.* **1979**, 978−982.
(23) Ciani, G.; Sironi, A.; Martinengo, S. *J. Chem. Soc., Dalton Trans.* **1981**, 519−523.
(24) Vidal, J. L.; Schoening, R. C. *J. Organomet. Chem.* **1981**, *218*, 217−227.
(25) Martinengo, S.; Ciani, G.; Sironi, A.; Chini, P. *J. Am. Chem. Soc.* **1978**, *100*, 7096−7098.
(26) Ciani, G.; Sironi, A.; Martinengo, S. *J. Organomet. Chem.* **1980**, *192*, C42−C46.
(27) Vidal, J. L.; Schoening, R. C. *Inorg. Chem.* **1981**, *20*, 265−269.
(28) Ciani, G.; Sironi, A.; Martinengo, S. *J. Chem. Soc., Dalton Trans.* **1982**, 1099−1102.
(29) Martinengo, S.; Ciani, G.; Sironi, A. *J. Chem. Soc., Chem. Commun.* **1980**, 1140−1141.
(30) Vidal, J. L.; Kapicak, L. A.; Troup, J. M. *J. Organomet. Chem.* **1981**, *215*, C11−C16.
(31) Ciani, G.; Magni, A.; Sironi, A.; Martinengo, S. *J. Chem. Soc., Chem. Commun.* **1981**, 1280−1282.
(32) Martinengo, S.; Ciani, G.; Sironi, A. *J. Am. Chem. Soc.* **1980**, *102*, 7564−7565.
(33) Vidal, J. L.; Schoening, R. C.; Troup, J. M. *Inorg. Chem.* **1981**, *20*, 227−238.
(34) Zanello, P. *Structure and Bonding*; Springer-Verlag: Berlin, 1992; Vol. 79, pp 101−213.
(35) Collini, D.; Femoni, C.; Iapalucci, M. C.; Longoni, G.; Svensson, P. H. *Inorg. Chim. Acta* **2003**, *350*, 321−328.

Table 1. IR Carbonyl Frequencies (cm^{-1}) in Acetonitrile of the Tetraethylammonium Salts of Rh Clusters Isolated in This Work

$[Rh_{14}(CO)_{25}]^{4-}$	1965s, 1933sh, 1809m, 1781sh
$[HRh_{14}(CO)_{25}]^{3-}$	1989s, 1964sh, 18m
$[Rh_{15}(CO)_{27}]^{3-}$	1993s, 1991s, 1837m, 1816sh
$[Rh_{15}(CO)_{25}(MeCN)_2]^{3-}$	1989s, 1887mw, 1853mbr, 1809mw
$[Rh_{17}(CO)_{30}]^{3-}$	2016s, 1999s, 1889mw, 1834mbr, 1779mw
$[Rh_{17}(CO)_{37}]^{3-}$	1993s, 1978sh, 1886mw, 1840mbr, 1812mw

Results and Discussion

1. Syntheses of $[H_{4-n}Rh_{14}(CO)_{25}]^{n-}$ (n = 3 and 4), $[Rh_{15}(CO)_{27}]^{3-}$, $[Rh_{15}(CO)_{25}(MeCN)_2]^{3-}$, $[Rh_{17}(CO)_{37}]^{3-}$, and $[Rh_{17}(CO)_{30}]^{3-}$ Clusters. As stated in the introduction, in the attempt to find a more selective synthesis of $[NiRh_{14}(CO)_{28}]^{4-}$,[35] we investigated the possible condensation of 2 equiv of $[Rh_7(CO)_{16}]^{3-}$ [36] with 1 equiv of Ni^{2+} ion. Somehow unexpectedly, the reaction led to the formation of the homometallic $[H_{4-n}Rh_{14}(CO)_{25}]^{n-}$ (n = 3 and 4) cluster. The best results have been obtained by adding ca. 1.5 equiv of $NiCl_2 \cdot 6H_2O$ per 1 mol of $[Rh_7(CO)_{16}]^{3-}$ salts in a tetrahydrofuran (THF) solution. The $[HRh_{14}(CO)_{25}]^{3-}$ trianion has been obtained in ca. 80% yields, owing to concomitant formation of some $[Rh_{12}(CO)_{30}]^{2-}$ and $[Rh(CO)_2Cl_2]^-$ side products. These salts have been separated by differential solubility in organic solvents, and $[NEt_4]_3[HRh_{14}(CO)_{25}]$ has been successfully crystallized from acetonitrile−hexane/diisopropyl ether mixtures. The corresponding $[Rh_{14}(CO)_{25}]^{4-}$ salt has been quantitatively prepared by deprotonation of $[HRh_{14}(CO)_{25}]^{3-}$ with potassium *tert*-butylate in anhydrous acetonitrile and crystallized by layering of diisopropyl ether, as previously reported.[28] The IR carbonyl absorptions of all relevant species are collected in Table 1.

It was unclear whether the oxidation of $[Rh_7(CO)_{16}]^{3-}$ to $[H_{4-n}Rh_{14}(CO)_{25}]^{n-}$ (n = 3 and 4) was to ascribe to the Ni^{2+}/Ni redox couple or the protonic acidity of coordinated water of the $[Ni(H_2O)_6]^{2+}$ aquo complex, which could enable reactions (1) and (2). The observed failure in including Ni atoms in the cluster frame and the absence of any detectable Ni metal were indicative of the latter explanation. To gain some better understanding of the above reaction, we investigated the redox aptitude of $[Rh_7(CO)_{16}]^{3-}$ by electrochemistry. As will be shown in section 3, the first oxidation of $[Rh_7(CO)_{16}]^{3-}$ occurs at −0.23 V vs SCE (formally, +0.04 V vs the hydrogen electrode) and is irreversible at any scan rate. Taking the standard redox potentials in water of the Ni^{2+}/Ni (−0.23 V) and $H^+/{}^1/_2H_2$ (0.0 V) couples as rough references (even if the pertinent potentials are not comparable and the redox couples are not in standard conditions), the $H^+/{}^1/_2H_2$ redox couple should be more effective. It seemed, therefore, reasonable to conclude that the Brønsted acidity of the $[Ni(H_2O)_6]^{2+}$ (pK_a = 9.9) aquo complex might give rise to protonation of the starting material to a very unstable $[HRh_7(CO)_{16}]^{2-}$ hydride derivative, which rapidly undergoes condensation via H_2 and CO elimination according to reaction (1). The observed formation of the $[HRh_{14}(CO)_{25}]^{3-}$ hydride derivative is in keeping with early reports that $[Rh_{14}(CO)_{25}]^{4-}$ is protonated even by water (equilibrium (2)).[25]

Scheme 1

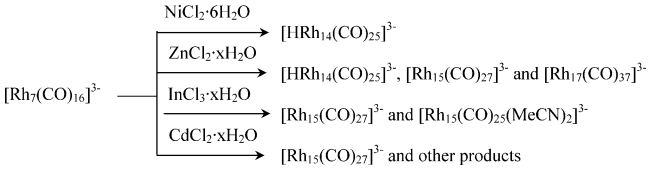

$$2[Rh_7(CO)_{16}]^{3-} + 2H^+ \rightarrow 2\{[HRh_7(CO)_{16}]^{2-}\} \rightarrow [Rh_{14}(CO)_{25}]^{4-} + H_2 + 7CO \quad (1)$$

$$[Rh_{14}(CO)_{25}]^{4-} + H^+ \rightleftarrows [HRh_{14}(CO)_{25}]^{3-} \quad (2)$$

The good selectivity of reaction (1) prompted the investigation of several other $[M(H_2O)_x]^{n+}$ aquo complexes with different pK_a's and M^{n+}/M potentials to further implement the above suggestion and to test the possibility of selectively obtaining some different Rh clusters by smoothly decreasing the pK_a. The experimental results are summarized in Scheme 1 and are roughly in keeping with the conclusion that aquo complexes, featuring $E°(M^{n+}/M)$ < ca. −0.20 V, do not lead to the formation of heterometallic Rh clusters, probably because of the inadequacy of their redox potentials relative to that of the $[Rh_7(CO)_{16}]^{3-/2-}$ redox couple. Such a conclusion also stems from the experimental observation that $SnCl_2 \cdot 2H_2O$ [pK_a = 3.4; $E°(Sn^{2+}/Sn)$ = −0.14 V], in spite of the relatively high Brønsted acidity, oxidizes $[Rh_7(CO)_{16}]^{3-}$ via the Sn^{2+}/Sn redox couple. Indeed, heterometallic rhodium−tin carbonyl clusters, such as $[Rh_{12}(\mu_{12}\text{-Sn})(CO)_{27}]^{4-}$ and $[Rh_{12}(\mu_{10}\text{-Sn})(CO)_{23}(\mu\text{-X})_2]^{4-}$ (X = Cl and Br), have been isolated in almost quantitative yields. These results will be reported elsewhere.[37]

In contrast, all investigated aquo complexes, featuring $E°(M^{n+}/M)$ < ca. −0.20 V, do not yield heterometallic but only homometallic Rh clusters. The charge/nuclearity ratio of the so far identified products is only very roughly in keeping with the pK_a of the pertinent aquo complex. Thus, as shown in Scheme 1, $ZnCl_2 \cdot xH_2O$ [pK_a = 9.0; $E°(Zn^{2+}/Zn)$ = −0.76 V], which is only slightly more acidic than $NiCl_2 \cdot 6H_2O$, affords a slightly more oxidized mixture of Rh clusters, which includes small amounts of the known $[H_{4-n}Rh_{14}(CO)_{25}]^{n-}$ and the new Rh-centered $[Rh_{15}(CO)_{27}]^{3-}$ and conjuncto $[Rh_{17}(CO)_{37}]^{4-}$ clusters. Although a cluster having the formula $[Rh_{15}(CO)_{27}]^{3-}$ has previously been reported,[25] the one isolated from this and the following reactions shows a significantly different metal skeleton and represents an isomer of the previously reported species obtained by pyrolysis (vide infra).

Adoption of a yet more acidic reagent, such as $InCl_3 \cdot xH_2O$ [pK_a = 4.0; $E°(In^{3+}/In)$ = −0.34 V], fairly selectively leads to $[Rh_{15}(CO)_{27}]^{3-}$ salts. However, this latter cluster has also been obtained in low yields upon the reaction of $[Rh_7(CO)_{16}]^{3-}$

(36) Chini, P.; Martinengo, S. *Chem. Commun*. **1969**, 1092−1093.

(37) Femoni, C.; Iapalucci, M. C.; Longoni, G.; Tiozzo, C.; Zacchini, S. *Dalton Trans.* **2007**, in press.

with $CdCl_2 \cdot xH_2O$ [pK_a = 10.1; $E°(Cd^{2+}/Cd) = -0.40$ V], even if the latter is the weakest Brønsted acid among those studied. This apparent disagreement may, perhaps, be due to the formation of a yet uncharacterized concomitant product.

Finally, the reaction of $[Rh_7(CO)_{16}]^{3-}$ with 1−2 equiv of a protonic acid, such as H_2SO_4, at room temperature affords a complex mixture of rhodium carbonyl clusters, from which only the known $[Rh_{17}(CO)_{30}]^{4-}$ has been so far isolated in poor yields. Similarly, the reaction in acetone of $[Rh_7(CO)_{16}]^{3-}$ with 2 equiv of CF_3SO_3H at 0 °C initially affords $[Rh_{14}(CO)_{25}]^{4-}$, which is then protonated by the further addition of 0.5 equiv to $[HRh_{14}(CO)_{25}]^{3-}$, according to eqs 1 and 2. The progressive addition of another 1 equiv of acid generates at least three other species with IR absorptions in the range 2040−2000 cm^{-1} for terminal and 1870−1840 cm^{-1} for bridges, whose characterization is in progress. Notice that the corresponding reaction with CF_3SO_3H at 0 °C has been earlier reported to give $[Rh_{14}(CO)_{26}]^{2-}$ in more than 85% yields.[24] On our working scale, it was impossible to calibrate with sufficient precision the tiny amount of required CF_3SO_3H acid and to add it in one shot. Perhaps, because of that, the reaction takes a different course.

All of the reported rhodium carbonyl clusters have been successfully separated by differential solubility of their $[NEt_4]^+$ salts, according to the procedures described in the Experimental Section. Most salts have been crystallized from acetone and isopropyl alcohol mixtures and characterized by IR, electrospray ionization mass spectrometry (ESI-MS), and X-ray diffraction analysis. During the above characterizations, it was noticed that acetonitrile solutions of $[Rh_{15}(CO)_{27}]^{3-}$ were slightly changing their IR pattern with time. Concomitantly, ESI-MS monitoring disclosed a progressive increase of the signal relative to the $[Rh_{15}(CO)_{25}]^{2-}$ ion, at the expense of those of $[Rh_{15}(CO)_{27}]^{2-}$ and $[Rh_{15}(CO)_{26}]^{2-}$. Crystallization of $[NEt_4]_3[Rh_{15}(CO)_{27}]$ from acetonitrile, rather than acetone, affords the carbonyl-substituted $[Rh_{15}(CO)_{25}(MeCN)_2]^{3-}$ trianion, which evidently arises from the substitution reaction (3).

$$[Rh_{15}(CO)_{27}]^{3-} + 2MeCN \rightarrow [Rh_{15}(CO)_{25}(MeCN)_2]^{3-} + 2CO \quad (3)$$

Attempts to reverse reaction (3), as well as to obtain the previously reported $[Rh_{15}(CO)_{30}]^{3-}$,[30] by exposure of $[Rh_{15}(CO)_{25}(MeCN)_2]^{3-}$ acetonitrile solutions to a carbon monoxide atmosphere resulted in degradation according to reaction (4). The $[Rh(CO)_{4-n}(MeCN)_n]^+$ (n = 1 and 2) species[38] have been identified by IR.

$$[Rh_{15}(CO)_{25}(MeCN)_2]^{3-} + (4-n)CO \rightarrow [Rh_{14}(CO)_{25}]^{4-} + [Rh(CO)_{4-n}(MeCN)_n]^+ + (2-n)MeCN \qquad (n = 1 \text{ and } 2) \quad (4)$$

Such a result complements the degradation of $[Rh_{15}(CO)_{27}]^{3-}$ with halide ions in acetonitrile to $[Rh_{14}(CO)_{25}]^{4-}$ and $[Rh(CO)_2X_2]^-$, through which $[H_{4-n}Rh_{14}(CO)_{25}]^{n-}$ (n = 3 and 4) salts have been originally prepared and characterized by Chini et al.[25]

2. X-ray Structures of $[NEt_4]_3[Rh_{15}(CO)_{27}]$, $[NEt_4]_3[Rh_{15}(CO)_{25}(MeCN)_2]\cdot 2MeCN$, and $[NEt_4]_3[Rh_{17}(CO)_{37}]$. As stated in the previous section, all Rh clusters isolated during this work, namely, $[NEt_4]_3[HRh_{14}(CO)_{25}]$, $[NEt_4]_4[Rh_{14}(CO)_{25}]$, $[NEt_4]_3[Rh_{15}(CO)_{27}]$, $[NEt_4]_3[Rh_{15}(CO)_{25}(MeCN)_2]\cdot 2MeCN$, $[NEt_4]_3[Rh_{17}(CO)_{30}]$, and $[NEt_4]_3[Rh_{17}(CO)_{37}]$, have been characterized by single-crystal X-ray diffraction studies. The structures of the $[HRh_{14}(CO)_{25}]^{3-}$, $[Rh_{14}(CO)_{25}]^{4-}$, and $[Rh_{17}(CO)_{30}]^{3-}$ clusters were found to be substantially identical with those already present in the literature. Therefore, their structures will not be reported here in any detail. We only report in some detail the structures of the $[Rh_{15}(CO)_{27}]^{3-}$, $[Rh_{15}(CO)_{25}(MeCN)_2]^{3-}$, and $[Rh_{17}(CO)_{37}]^{3-}$ trianions.

$[NEt_4]_3[Rh_{15}(CO)_{27}]$. The unit cell of the $[NEt_4]_3[Rh_{15}(CO)_{27}]$ salts contains two pairs of independent $[Rh_{15}(CO)_{27}]^{3-}$ cluster anions and 12 $[NEt_4]^+$ cations separated by normal van der Waals contacts. The two independent $[Rh_{15}(CO)_{27}]^{3-}$ ions only slightly differ in their carbonyl stereochemistry. Thus, one terminal carbonyl group and one bridging carbonyl group of the first ion are split into two positions with refined occupancy fractions of 0.66 (C26−O26 and C27−O27) and 0.33 (C260−O260 and C270−O270), respectively. Therefore, only the structure of the ordered ion with the adopted numbering scheme is shown in Figure 1. The average bond distances of both ions (as well as those of the structurally related $[Rh_{15}(CO)_{25}(MeCN)_2]^{3-}$ cluster) are collected in Table 2. A complete list of all interatomic distances is given in the Supporting Information (Table S1). As shown in Figure 1, the metal framework of $[Rh_{15}(CO)_{27}]^{3-}$ consists of a slightly distorted chunk of a body-centered-cubic metal lattice. Notice that in this and the following structures both Rh−Rh and Rh−C contacts are rather scattered (see Tables S1−S3 in the Supporting Information). The almost continuous variation in lengths makes it difficult to decide where to cut. Therefore, we have taken the arbitrary decision to show as bonds in Figures 1 and 2 only those within a ca. 20% increase of the shortest Rh−Rh and Rh−C contacts. The drawn Rh−Rh contacts agree fairly well with a description of the metal frame as a hexacapped centered cube of Rh atoms. The major distortion is that one edge of the cube (Rh23−Rh27) is beyond the chosen limit (being elongated beyond 3.25 Å). Almost as a consequence, the corresponding Rh31 and Rh32 caps shrink closer to the four Rh atoms of the corresponding square faces and the unique interstitial Rh21 atom. From a formal point of view, the structure of this cluster derives from that of $[Rh_{14}(CO)_{25}]^{4-}$ by capping the unique uncapped square face with a $[Rh(CO)_2]^+$ moiety, according to the right side of the pictorial representation given in Scheme 2. As a result, the present isomer A of $[Rh_{15}(CO)_{27}]^{3-}$ exhibits a metal framework very

(38) Prater, M. E.; Pence, L. E.; Clérac, R.; Finnis, G. M.; Campana, C.; Auban-Senzier, P.; Jérome, D.; Canadell, E.; Dunbar, K. R. *J. Am. Chem. Soc.* **1999**, *121*, 8005−8016.
(39) Ceriotti, A.; Della Pergola, R.; Garlaschelli, L.; Longoni, G.; Manassero, M.; Ma sciocchi, N.; Sansoni, M.; Zanello, P. *Gazz. Chim. Ital.* **1992**, *122*, 365−371.

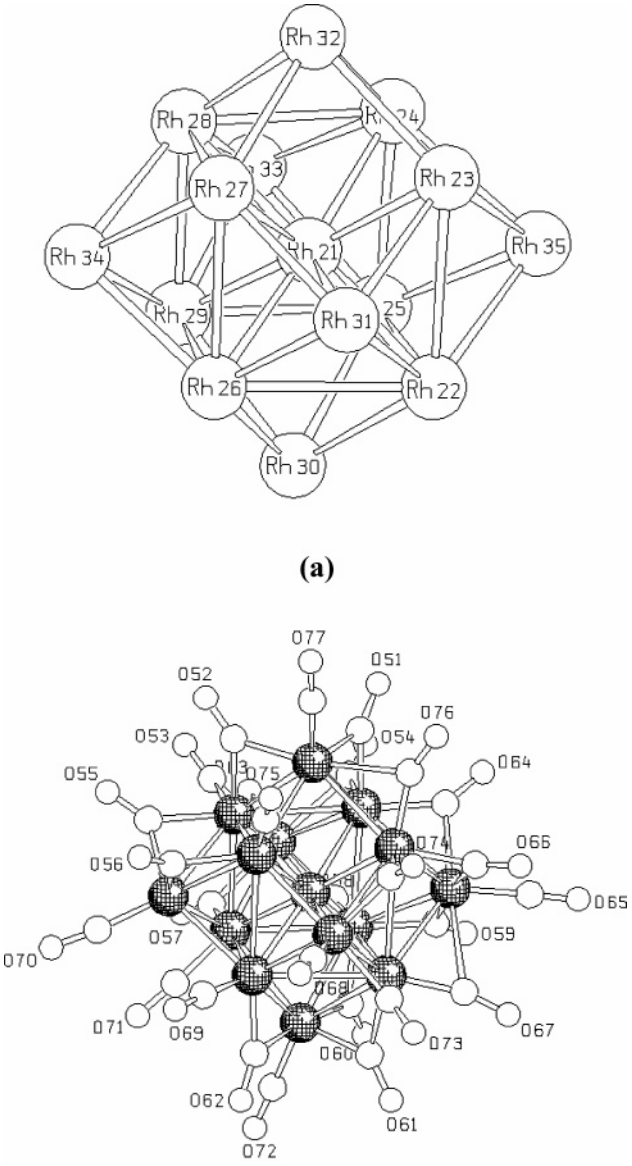

Figure 1. X-ray structure of the ordered $[Rh_{15}(CO)_{27}]^{3-}$ trianion (only one of the two independent anions present in the unit cell is represented): (a) rhodium framework with a numbering scheme; (b) whole structure with numbering of O atoms (C atoms are numbered as the corresponding O atoms).

Table 2. Average Bonding Distances (Å) in the Two Independent Ions of $[Rh_{15}(CO)_{27}]^{3-}$ and $[Rh_{15}(CO)_{25}(MeCN)_2]^{3-}$

	$[Rh_{15}(CO)_{27}]^{3-}$		
	first ion	second ion	$[Rh_{15}(CO)_{25}(MeCN)_2]^{3-}$
$Rh_{interstitial}-Rh_{cube}$	2.619	2.607	2.600
$Rh_{cube}-Rh_{cube}$	3.022	3.009	3.000
$Rh_{cube}-Rh_{cap}$	2.762	2.766	2.756
$Rh-C_{terminal}$	1.852	1.857	1.847
$Rh-C_{edge-bridging}$	2.023	2.035	2.031
$C-O_{terminal}$	1.143	1.141	1.146
$C-O_{edge-bridging}$	1.171	1.162	1.174
Rh−N			2.110

similar to that of previously reported $[Rh_{15}(CO)_{30}]^{3-}$ and only differs in the number and stereochemistry of the carbonyl groups. Moreover, its structure is a variation of that of the previously reported $[Rh_{15}(CO)_{27}]^{3-}$ species, isolated from the

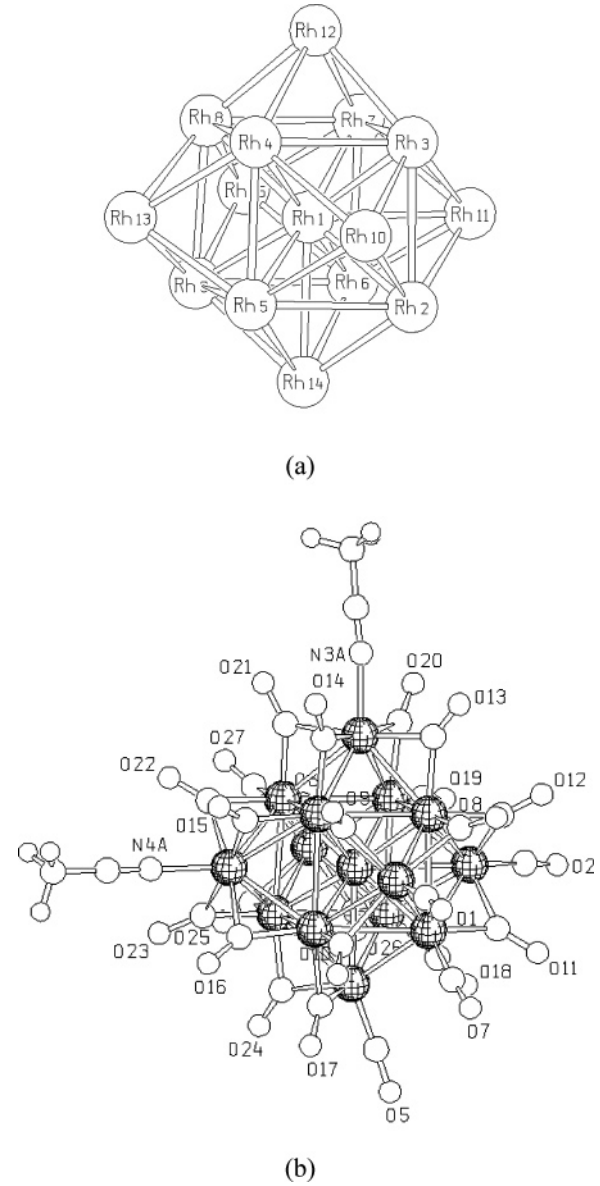

Figure 2. X-ray structure of the $[Rh_{15}(CO)_{25}(MeCN)_2]^{3-}$ trianion: (a) rhodium framework with a numbering scheme; (b) whole structure with numbering of O atoms (C atoms are numbered as the corresponding O atoms).

mixture of products obtained by pyrolysis under nitrogen of $Rh_4(CO)_{12}$ and NaOH in isopropyl alcohol.[25] The published metal frame of $[Rh_{15}(CO)_{27}]^{3-}$ may also be derived from $[Rh_{14}(CO)_{25}]^{4-}$ by capping with a $[Rh(CO)_2]^+$ moiety and corresponds to isomer B. As shown on the left side of Scheme 2, condensation to give isomer B should formally occur onto a concave face generated by two Rh atoms capping two adjacent square faces of the Rh-centered cube. The formation of isomer A may stem from the milder conditions of our synthesis and/or the use of reagents, which may behave both as Brønsted and Lewis acids. For instance, if a Lewis acid blocks the more basic concave face, as it does H^+ in $[HRh_{14}(CO)_{25}]^{3-}$, an entering $[Rh(CO)_2]^+$ moiety may be addressed to condense onto the free square face of the cube. The decreased negative charge of the cluster may then lead to dissociation of the Lewis acid ($M^{II}Cl_2$ or H^+)/Lewis base ($[Rh_{14}(CO)_{25}]^{4-}$) adduct and give rise to isomer

Scheme 2

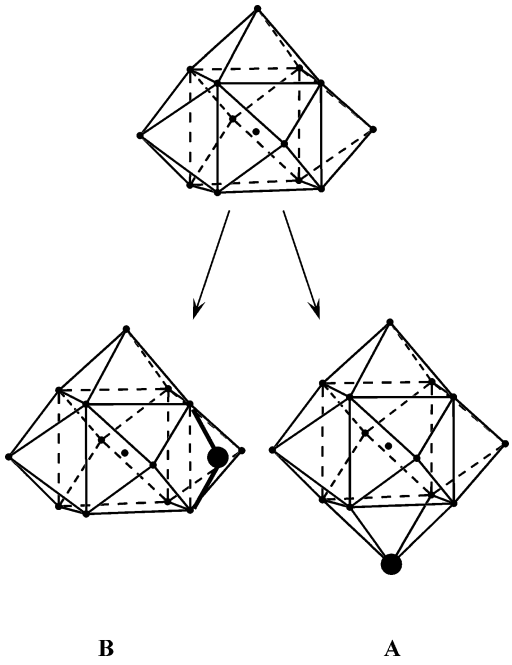

A. The alternative suggestion that isomerization is due to the different packing forces of the $[NMe_4]^+$ and $[NEt_4]^+$ salts of $[Rh_{15}(CO)_{27}]^{3-}$ seems less likely. Attempts to convert isomer A into isomer B by thermal treatment have so far been unsuccessful.

$[NEt_4]_3[Rh_{15}(CO)_{25}(MeCN)_2]\cdot 2MeCN$. The structure of the $[Rh_{15}(CO)_{25}(MeCN)_2]^{3-}$ trianion with a numbering scheme is shown in Figure 2. The average interatomic distances are collected in Table 2. The full list of bonding interactions is given in the Supporting Information as Table S2. As shown in Figure 2, the overall structure is very similar to that of the parent isomer A of $[Rh_{15}(CO)_{27}]^{3-}$. The major differences between the two are found in the ligand stereochemistry. First of all, the terminal carbonyl ligands of two adjacent capping Rh atoms have been substituted by two acetonitrile molecules. Perhaps significantly, the ligand-substituted caps are both trans to the two Rh caps shrinking closer to the interstitial Rh atom. Second, these two capping Rh atoms are now surrounded by four edge-bridging carbonyl groups. As a consequence, two vertices of the cube are no longer bonded to terminal ligands because of their conversion into bridges. The terminal-to-bridge conversion of one carbonyl group for each substituted cap is clearly related to the presence of a less π-acidic ligand, such as MeCN. To our knowledge, $[Rh_{15}(CO)_{25}(MeCN)_2]^{3-}$ represents a very rare example of a high-nuclearity anionic cluster in which carbonyl groups are substituted by acetonitrile ligands. To the best of our knowledge, the only previous example is $[Co_6Ni_2C_2(CO)_{14}(MeCN)_2]^{2-}$,[39] although several neutral carbonyl clusters containing this same ligand are known, e.g., $Os_3(CO)_{11}(MeCN)$,[40] $Ru_5C(CO)_{15}(MeCN)$,[41] and $CuRh_9(CO)_{19}(MeCN)_3$.[42] Carbonyl-substituted anionic clusters involving more π-acidic ligands such as pyridine or triphenylphosphine are more common, e.g., $[Rh_5(CO)_{13}Py_2]^-$,[43] $[Pd_{29}(CO)_{28}(PPh_3)_7]^{2-}$,[44] and $[Pd_{33}Ni_9(CO)_{41}(PPh_3)_6]^{4-}$.[45] Beyond other considerations, the reported $[Rh_{15}(CO)_{25}(MeCN)_2]^{3-}$ here may represent a valuable starting material for cluster networking, for instance, by substitution of the monodentate acetonitrile with bidentate ligands. Though its structure was initially determined on a crystal found in one of the earlier experiments,[2] the lack of a reliable synthesis hindered the development of its chemistry. Its rational synthesis, according to eq 3, now enables cluster networking experiments, which are in progress.

$[NEt_4]_3[Rh_{17}(CO)_{37}]$. The crystal structure of $[NEt_4]_3[Rh_{17}(CO)_{37}]$ consists of ionic packing of $[Rh_{17}(CO)_{37}]^{3-}$ cluster trianions and $[NEt_4]^+$ cations separated by normal van der Waals contacts. The structure of the trianion with a numbering scheme is shown in Figure 3, and the average interatomic distances are collected in Table 3. The full list of bonding interactions is given in the Supporting Information as Table S3. As shown in Figure 3, the metal framework of $[Rh_{17}(CO)_{37}]^{3-}$ is derived by joining with a Rh−Rh bond two cluster moieties. B−B conjuncto boranes are rather common, whereas M−M conjuncto metal clusters are rather rare. To our knowledge, the only known examples are $[Rh_{12}(CO)_{30}]^{2-}$ [46,47] and $[Ir_8(CO)_{22}]^{2-}$,[48] which have been reported in the early days of metal carbonyl cluster chemistry. These are based on two identical Rh_6 and Ir_4 moieties, respectively, joined together by a M−M bond. In this regard, the $[Rh_{17}(CO)_{37}]^{3-}$ cluster is unique in that it is derived by joining together two different cluster moieties: a Rh_6 octahedron and a Rh_{11} truncated trigonal bipyramid of frequency 2. The Rh−Rh bond [Rh6−Rh7 = 2.744(1) Å] joining the two moieties is spanned by two μ-CO ligands (Rh−C = 1.935 Å, on average), as for the related $[Rh_{12}(CO)_{30}]^{2-}$. By the formal assignment of one μ-CO ligand to each moiety, $[Rh_{17}(CO)_{37}]^{3-}$ may be considered to be derived by coupling of $[Rh_6(CO)_{15}]^{\bullet-}$ and $[Rh_{11}(CO)_{22}]^{\bullet 2-}$ radical anions. The carbonyl stereochemistry of the octahedral $[Rh_6(CO)_{11}(\mu_3\text{-}CO)_4]^{\bullet-}$ moiety comprises 11 terminal ligands (2 per each Rh atom but the one bonded to the Rh_{11} moiety) and 4 face-bridging carbonyl groups on alternating faces of the octahedron. Such a stereochemistry is identical with that of the related moiety of $[Rh_{12}(CO)_{30}]^{2-}$.[47] The Rh−Rh distances within the octahedral moiety are rather scattered and range from 2.479(1) to 3.140(1) Å.

(40) Johnson, B. F. G.; Lewis, J.; Pippard, D. A. *J. Chem. Soc., Dalton Trans.* **1981**, 407−412.
(41) Johnson, B. F. G.; Lewis, J.; Nicholls, J. N.; Puga, J.; Raithby, P. R.; Rosales, M. J.; McPartlin, M.; Clegg, W. *J. Chem. Soc., Dalton Trans*. **1983**, 277−285.
(42) Ciani, G.; Moret, M.; Fumagalli, A.; Martinengo, S. *Inorg. Chem.* **1989**, *28*, 2011−2013.
(43) Facchinetti, G.; Funaioli, T.; Zanazzi, P. F. *J. Organomet. Chem*. **1993**, *460*, C34−C36.
(44) Kawano, M.; Bacon, J. W.; Campana, C. F.; Winger, B. E.; Dudek, J. D.; Sirchio, S. A.; Scruggs, S. L.; Geiser, U.; Dahl, L. F. *Inorg. Chem*. **2001**, *40*, 2554−2569.
(45) Kawano, M.; Bacon, J. W.; Campana, C. F.; Dahl, L. F. *J. Am. Chem. Soc*. **1996**, *118*, 7869−7870.
(46) Chini, P.; Martinengo, S. *Inorg. Chim. Acta* **1969**, 299−302.
(47) Albano, V. G.; Bellon, P. L. *J. Organomet. Chem*. **1969**, *19*, 405−415.
(48) Demartin, F.; Manassero, M.; Sansoni, M.; Garlaschelli, L.; Raimondi, C. C.; Martinengo, S.; Canziani, F. *J. Chem. Soc., Chem. Commun.* **1981**, 528−529.

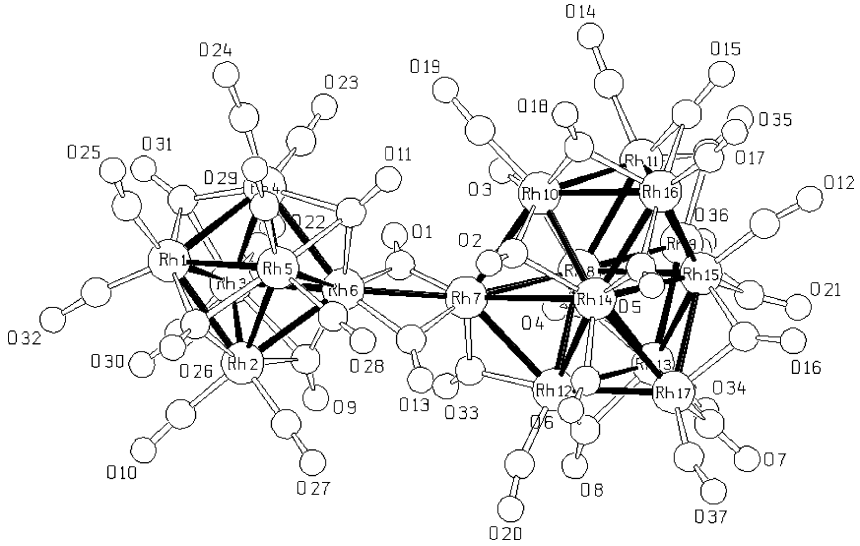

Figure 3. X-ray structure of the $[Rh_{17}(CO)_{17}(\mu\text{-}CO)_{10}(\mu_3\text{-}CO)_{10}]^{3-}$ trianion with a numbering scheme (C atoms are numbered as the corresponding O atoms).

Table 3. Average Bonding Distances (Å) in $[Rh_{17}(CO)_{37}]^{3-}$

$Rh-Rh_{octahedral\ moiety}$	2.773	$Rh-C_{face-bridging}$	2.223
$Rh-Rh_{trunc.\ trigonal\ bipyramid}$	2.783	$C-O_{terminal}$	1.153
$Rh-Rh_{junction}$	2.740	$C-O_{edge-bridging}$	1.170
$Rh-C_{terminal}$	1.864	$C-O_{face-bridging}$	1.165
$Rh-C_{edge-bridging}$	2.047		

In contrast, the metal frame of the $[Rh_{11}(CO)_{12}(\mu\text{-}CO)_5(\mu_3\text{-}CO)_5]^{\bullet 2-}$ moiety is significantly different from that of the known $[Rh_{11}(CO)_{23}]^{3-}$ cluster[49] and consists of a chunk of hcp metal lattice related to that featured by $[H_{4-n}Ni_{12}(CO)_{21}]^{n-}$ ($n = 2-4$).[50,51] The reported $[Rh_{11}(CO)_{23}]^{3-}$ cluster has been suggested to be derived formally from the metal frame of $[Rh_{10}(CO)_{21}]^{2-}$ by condensation of a $Rh(CO)_2$ fragment on a convex bistriangular face, followed by some rearrangement to give rise to three fused octahedrons, as shown in Scheme 3(A).[52] The present $[Rh_{11}(CO)_{22}]^{\bullet 2-}$ moiety may be likewise derived from $[Rh_{10}(CO)_{21}]^{2-}$ [52] by condensation of a Rh(CO) moiety on one of its two concave bistriangular faces, as shown in Scheme 3(B).

The Rh−Rh bonds of the $[Rh_{11}(CO)_{22}]^{\bullet 2-}$ moiety are comprised of a slightly narrower range [2.657(1)−3.082(1) Å] than that of the $[Rh_6(CO)_{11}(\mu_3\text{-}CO)_4]^{\bullet -}$ moiety. As far as the CO stereochemistry is concerned, each Rh atom of the two outer triangles is bonded to one terminal and two edge-bridging ligands (one spanning one edge of the triangle and the second spanning an interlayer interaction). Of the five Rh atoms of the inner layer, three are bonded to two edge-bridging CO ligands as the one joined to the Rh_6 moiety. The fifth Rh atom is bonded to one terminal and two edge-bridging ligands. In the above description, we have included all Rh−C contacts in the 1.9−2.30 Å range and excluded longer contacts.

Scheme 3

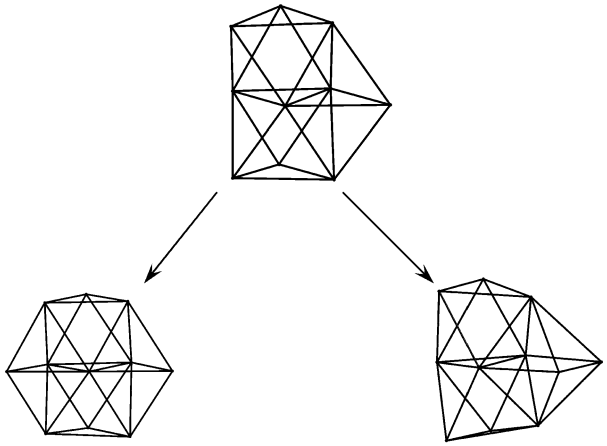

B **A**

3. Electrochemical Studies of $[Rh_7(CO)_{16}]^{3-}$, $[H_3Rh_{13}(CO)_{24}]^{2-}$, $[HRh_{14}(CO)_{25}]^{3-}$, and $[Rh_{15}(CO)_{27}]^{3-}$. Electrochemical investigations have been carried out on $[Rh_7(CO)_{16}]^{3-}$ and the Rh-centered $[H_3Rh_{13}(CO)_{24}]^{2-}$, $[HRh_{14}(CO)_{25}]^{3-}$, and $[Rh_{15}(CO)_{27}]^{3-}$.

As shown in Figure 4a, $[Rh_7(CO)_{16}]^{3-}$ undergoes a reduction process ($E^{\circ\prime} = -1.67$ V vs SCE), having features of partial chemical reversibility (in fact, the i_{pa}/i_{pc} ratio progressively increases from 0.4 to 0.6 upon an increase of the scan rate from 0.02 to 2.0 V s^{-1}), as well as a main irreversible oxidation ($E_p = -0.23$ V), followed, in turn, by a series of further ill-defined oxidation steps. In reality, as shown in Figure 4b, not only does the increase of the scan rate cause the disappearance of the most anodic processes (which are, hence, assigned to byproducts arising from chemical complications following the first anodic process) but also a second irreversible oxidation process appears ($E_p = +0.60$ V), which likely arises from the original trianion.

(49) Fumagalli, A.; Martinengo, S.; Ciani, G.; Sironi, A. *J. Chem. Soc., Chem. Commun*. **1983**, 453−454.
(50) Broach, R. W.; Dahl, L. F.; Longoni, G.; Chini, P.; Schultz, A. J.; Williams, J. M. *Adv. Chem. Ser*. **1978**, *167*, 93−110.
(51) Barkley, J. V.; Heaton, B. T.; Manzi, L.; Smith, A. K.; Steiner, A.; Nakayama, H.; Miyagi, K.; Harding, R.; Eguchi, T.; Longoni, G. *J. Organomet. Chem*. **1999**, *573*, 254−260.
(52) Martinengo, S.; Ciani, G.; Sironi, A. *J. Chem. Soc., Chem. Commun*. **1986**, 1282−1283.

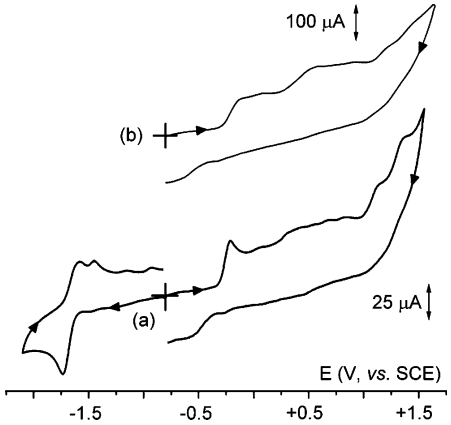

Figure 4. Cyclic voltammetric responses recorded at a glassy carbon electrode in a MeCN solution of $[Rh_7(CO)_{16}]^{3-}$ (1.3×10^{-3} mol dm^{-3}). $[NEt_4][PF_6]$ (0.1 mol dm^{-3}) is the supporting electrolyte. Scan rates: (a) 0.2 V s^{-1}; (b) 2 V s^{-1}.

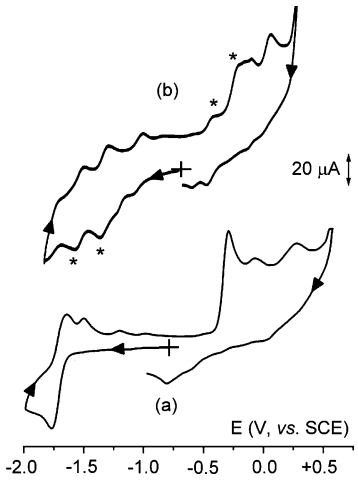

Figure 5. Cyclic voltammetric profiles recorded at a platinum electrode in a MeCN solution of (a) $[Rh_7(CO)_{16}]^{3-}$ (2.2×10^{-3} mol dm^{-3}) and (b) after exhaustive one-electron oxidation at the first anodic process (see the text). $[NEt_4][PF_6]$ (0.1 mol dm^{-3}) is the supporting electrolyte. Scan rate: 0.2 V s^{-1}.

The remarkable instability of the $[Rh_7(CO)_{16}]^{(3-n)-}$ ($n = 1$ and 2; see later) anions is proven by the substantial lack of directly associated responses in the backscans at high scan rate.

Controlled potential coulometry in correspondence of the first oxidation ($E_w = -0.15$ V) consumed one electron *per* molecule (in reality 1.1 electrons *per* molecule, likely because of the partial involvement of the minor byproduct, which affords a very close anodic process). In this connection, it is useful to look at the cyclic voltammetric profile recorded on the exhaustively one-electron-oxidized solution (see Figure 5). A series of new processes appear with respect to the original profile. In particular, we note that the starred peak systems are strongly reminiscent of the cyclic voltammetric fingerprint of $[HRh_{14}(CO)_{25}]^{3-}$ (compare with Figure 7 and the pertinent discussion), thus supporting the chemical findings discussed in section 1. Further unidentified species are also present. The formal electrode potentials of the above-discussed redox processes are compiled in Table 4, together with those of the chemically related $[HRh_{14}(CO)_{25}]^{3-}$ species, which will be discussed later.

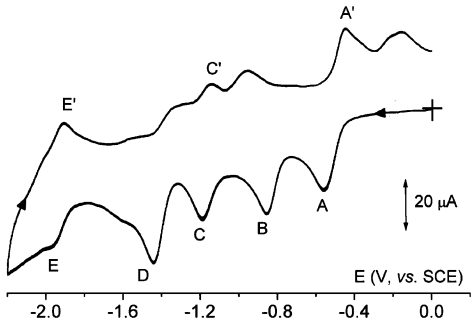

Figure 6. Cyclic voltammogram recorded at a platinum electrode in a MeCN solution of $[H_3Rh_{13}(CO)_{24}]^{3-}$ (1.5×10^{-3} mol dm^{-3}). $[NEt_4][PF_6]$ (0.1 mol dm^{-3}) is the supporting electrolyte. Scan rate: 0.2 V s^{-1}.

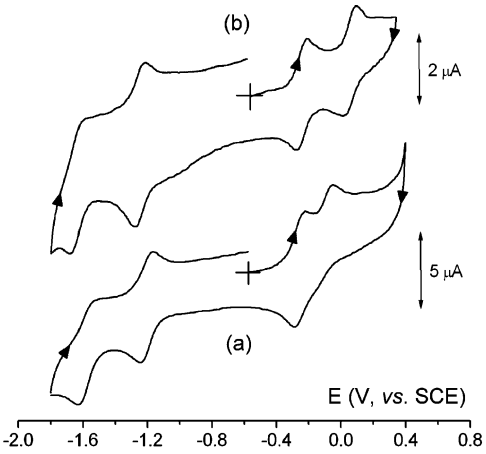

Figure 7. Cyclic voltammograms recorded at a platinum electrode in (a) a MeCN solution of $[HRh_{14}(CO)_{25}]^{3-}$ (0.6×10^{-3} mol dm^{-3}) and (b) a DMF solution of $[HRh_{14}(CO)_{25}]^{3-}$ (0.4×10^{-3} mol dm^{-3}). $[NEt_4][PF_6]$ (0.1 mol dm^{-3}) is the supporting electrolyte. Scan rate: 0.2 V s^{-1}.

As illustrated in Figure 6, the hcp $[H_3Rh_{13}(CO)_{24}]^{2-}$ cluster dianion undergoes the sequential reductions A, B, C, D, E, to which only the reoxidations E′, C′, and A′ look like they are directly associated in the backscan. Controlled potential coulometry in correspondence with the first reduction ($E_w = -0.6$ V) consumes about 0.8 electrons *per* molecule, thus supporting the one-electron nature of the process. Analysis of the cyclic voltammetric response pertinent to such a reduction with scan rates varying from 0.02 to 1.00 V s^{-1} suggests that the process is diffusion-controlled and complicated by a relatively slow first-order, reversible chemical reaction (E_rC_r mechanism).[53] In fact, (i) the current function $i_{pc}v^{-1/2}$ is maintained substantially constant, (ii) the current ratio i_{pa}/i_{pc} progressively decreases from 0.82 to 0.56, and (iii) the peak-to-peak separation remains constant and amounts to ca. 60 mV.

In view of the roughly similar heights of peaks B, C, and E, these are also assigned as one-electron processes. In contrast, peak D arises from chemical complications following the preceding processes in that not only does it tend to decrease upon increase in the cyclic voltammetric scan rate but also the solution resulting from the above-cited exhaustive reduction displays the peak systems A′/A and E/E′ interposed by a higher amount of the (unidentified) byproduct

(53) Zanello, P. *Inorganic Electrochemistry. Theory, Practice and Application*; RSC Books: Cambridge, U.K., 2003.

Table 4. Formal Electrode Potentials (V vs SCE) and Peak-to-Peak Separations (mV) for the Redox Processes Exhibited by the Rh Clusters $[Rh_7(CO)_{16}]^{3-}$ and $[HRh_{14}(CO)_{25}]^{3-}$

	reduction processes				oxidation processes				
compound	$E^{\circ\prime}_{first}$	ΔE_p[a]	$E^{\circ\prime}_{second}$	ΔE_p[a]	$E^{\circ\prime}_{first}$	ΔE_p[a]	$E^{\circ\prime}_{second}$	ΔE_p[a]	solvent
$[Rh_7(CO)_{16}]^{3-}$	−1.67	103			−0.23[a,b]		+0.60[b,c]		MeCN
$[HRh_{14}(CO)_{25}]^{3-}$	−1.25	90	−1.58[d]	110	−0.25	90	−0.02[b,e]		MeCN
	−1.22	85	−1.63[d]	75	−0.26	80	+0.08	68	DMF

[a] Measured at 0.1 V s^{-1}. [b] Peak-potential value. [c] Measured at 2.00 V s^{-1}. [d] Partial chemical reversibility. [e] Difficult to determine (see the text).

Table 5. Formal Electrode Potentials (V vs SCE) and Peak-to-Peak Separations (mV) for the Reduction Processes Exhibited by the Rh Clusters $[H_3Rh_{13}(CO)_{24}]^{3-}$ and $[Rh_{15}(CO)_{27}]^{3-}$ in a MeCN Solution

compound	$E^{\circ\prime}_{first}$	ΔE_p[a]	$E^{\circ\prime}_{second}$	ΔE_p[a]	$E^{\circ\prime}_{third}$	ΔE_p[a]	$E^{\circ\prime}_{fourth}$	ΔE_p[a]
$[H_3Rh_{13}(CO)_{24}]^{3-}$	−0.53	60	−0.84[a,b]		−1.17	58	−1.95	*c*
$[Rh_{15}(CO)_{27}]^{3-}$	−0.63[d]	*c*	−1.48	90	−1.79	65	−2.29d	*c*

[a] Measured at 0.1 V s^{-1}. [b] Peak-potential value. [c] Difficult to determine. [d] From Osteryoung square-wave voltammetry.

responsible for peak D. In addition, the chemical complications associated with peak B make the peak system C/C′ a little intense at low scan rate, whereas it increases in intensity by an increase of the scan rate. The formal electrode potentials of the mentioned redox processes are compiled in Table 5, together with those of $[Rh_{15}(CO)_{27}]^{3-}$, which will be discussed later.

The body-centered $[HRh_{14}(CO)_{25}]^{3-}$ trianion undergoes two oxidations and two reductions, all possessing features of chemical reversibility (see Figure 7). A further, partially reversible, multielectron oxidation (not shown in the figures) is also present in both cases at higher potential values (>+0.4 V). Analysis of the cyclic voltammetric responses with the scan rate indicates that both the first oxidation and the first reduction are chemically reversible on the cyclic voltammetric time scale. In contrast, the second oxidation in a MeCN solution is too close to the first process to allow a detailed analysis, whereas in a *N*,*N*-dimethylformamide (DMF) solution, the results are only partially chemically reversible, as happens for the most cathodic reduction in both solvents.

Attempts to determine the number of electrons involved in the aforementioned redox processes were unsuccessful, probably because of the very low currents consistent with the limited solubility of the complex. As a matter of fact, the consumption of 0.3 electrons *per* molecule in correspondence with the first oxidation in a DMF solution required about 1 h. The only indication from such a measurement is that the partially oxidized solution has a cyclic voltammetric behavior quite similar to the original one, thus confirming that no detectable degradation occurred. In this picture, we assume that all of the processes involve one-electron transfers, and their redox potentials are compiled in Table 4.

As illustrated in Figure 8a, the body-centered $[Rh_{15}(CO)_{27}]^{3-}$ in a MeCN solution undergoes a sequence of reduction processes, which possess features of chemical reversibility in cyclic voltammetry only at relatively high scan rates. The occurrence of slow chemical complications following the different electron transfers is clearly supported by the OSWV voltammogram shown in Figure 8b. As discussed in section 1, the chemical complications may easily arise from carbonyl substitution reactions, which lead to the formation of

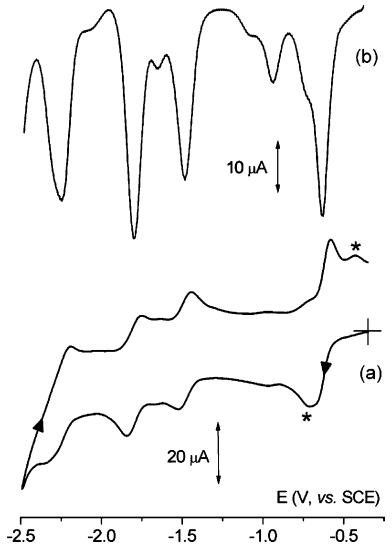

Figure 8. Cyclic (a) and Osteryoung square-wave (b) voltammograms recorded at a mercury electrode in a MeCN solution of $[Rh_{15}(CO)_{27}]^{3-}$ (0.9×10^{-3} mol dm^{-3}). $[NEt_4][PF_6]$ (0.1 mol dm^{-3}) is the supporting electrolyte. Scan rates: (a) 0.5 V s^{-1}; (b) 0.1 V s^{-1}.

$[Rh_{15}(CO)_{25}(MeCN)_2]^{3-}$. Unfortunately, the low solubility of $[NEt_4]_3[Rh_{15}(CO)_{27}]$ salt in acetone, in the presence of supporting electrolytes, hampered parallel studies in this solvent.

Because we did not succeed in determining the number of electrons involved in the redox processes in that the electrolysis current decayed very slowly, probably because of the continuous electrogeneration of redox-active byproducts, we naively assign all of the different electron additions as one-electron processes (in fact, the apparent higher peak height of the first reduction is attributed to the overlapping of the starred peak system, which tends to disappear upon an increase of the scan rate).

4. Conclusions. As a result of the reported experiments, it may be concluded that several high-nuclearity rhodium carbonyl clusters can be fairly selectively obtained by redox condensation of preformed rhodium carbonyl clusters with species in different oxidation states generated in situ by the $H^+/^1/_2H_2$ redox couple deriving from the Brønsted acidity of water coordinated to M^{2+} or M^{3+} metal ions. In some cases, that enables a better control of the reaction than that obtainable with strong protonic acids. The very mild

experimental conditions (0−25 °C, 1 atm), which can be adopted, enable isolation of either isomers of some previously reported cluster or new carbonyl-rich species, which were not previously detected. Moreover, isolation of an isomeric $[Rh_{15}(CO)_{27}]^{3-}$, which displays the same metal framework as that of the nonisoelectronic $[NiRh_{14}(CO)_{28}]^{4-}$ and $[Rh_{15}(CO)_{30}]^{3-}$ species, definitely proves that a given metal framework can be stabilized with a varying number of cluster valence electrons.

It seems also fair to conclude that an interstitial Rh atom is less effective than Ni, Pt, or Ag in promoting redox behavior and multivalence in their carbonyl clusters. The reason is probably electronic and, perhaps, descends from the relative energy of the valence d orbitals of Rh in comparison to those of Ni and Pt. Indeed, it has been suggested that every time the d orbitals of the interstitial metal atom are sufficiently low in energy with respect to the molecular orbitals of suitable symmetry of the cage, some antibonding combination may fall in the frontier region and lead to exceptional electron count and a prelude to nanocapacitor behavior.[6,54] Being safely predictable that Rh−Rh interactions are stronger than Ni−Rh interactions, the strengthening effect of the metal frame alone cannot justify either the upsurge of chemically reversible redox behavior or the fact that, of the $[HRh_{14}(CO)_{25}]^{3-}$ and $[Ni_5Rh_9(CO)_{25}]^{3-}$ pair of isostructural clusters, only the latter is multivalent and the corresponding oxidized $[Ni_5Rh_9(CO)_{25}]^{2-}$ species has been isolated.[9] However, it should be taken into account that the lack of chemical reversibility of several electrochemical redox changes of the so far investigated Rh species could be due to the polyhydride nature of some samples or the instability toward CO substitution of some other compounds. For instance, the presence of two or more hydride atoms could favor elimination of molecular H_2 upon reduction. On the other side, a relatively high negative charge and a distinguished affinity of hydride atoms for a polycavity Rh cluster would favor protonation by traces of water. All of the above side processes are potentially detrimental for electrochemical reversibility and may hamper observation of multivalence.

Experimental Section

All reactions including sample manipulations were carried out with standard Schlenk techniques under nitrogen and in carefully dried solvents. The $[Rh_7(CO)_{16}]^{3-}$ salts were prepared according to the literature.[36] The $[H_3Rh_{13}(CO)_{24}]^{2-}$ cluster dianion has been prepared by mild pyrolysis of mixtures of $Rh_4(CO)_{12}$ and NaOH in isopropyl alcohol and under a hydrogen atmosphere, according to the procedure described in ref 55, and isolated as a $[NEt_4]^+$ salt.

Analyses of Rh have been performed by atomic absorption on a Pye-Unicam instrument. Analyses of C, H, and N were obtained with a ThermoQuest FlashEA 1112NC instrument. IR spectra were recorded on a Perkin-Elmer Spectrum One interferometer using CaF_2 cells. Electron paramagnetic resonance experiments were carried out on a Bruker ER 041 XG instrument. NMR spectra were recorded on a Varian 400 MHz instrument and ESI-MS on a Waters ZQ4000/ZMD instrument.

Anhydrous (≥99.5%) acetonitrile (MeCN) and (≥99.8%) *N*,*N*-dimethylformamide (DMF) solvents were Fluka products. Fluka $[NBu_4][PF_6]$ (electrochemical grade) was used as the supporting electrolyte (0.2 mol dm^{-3}). Cyclic voltammetry was performed in a three-electrode cell containing a platinum working electrode surrounded by a platinum-spiral counter electrode and an aqueous saturated calomel reference electrode (SCE) mounted with a Luggin capillary. A BAS 100 W electrochemical analyzer was used as the polarizing unit. All of the potential values are referred to the SCE. Under the present experimental conditions, the one-electron oxidation of ferrocene occurs at $E^{\circ\prime} = +0.38$ V in a MeCN solution and at $E^{\circ\prime} = +0.47$ V in a DMF solution. Controlled potential coulometry was performed in an H-shaped cell with anodic and cathodic compartments separated by a sintered-glass disk. The working macroelectrode was a platinum gauze; a mercury pool was used as the counter electrode. Structure drawings have been done with *SCHAKAL99*.[56]

Synthesis of $[HRh_{14}(CO)_{25}]^{3-}$ from $[Rh_7(CO)_{16}]^{3-}$ and $NiCl_2\cdot 6H_2O$. A suspension of $NiCl_2\cdot 6H_2O$ (0.038 g, 0.144 mmol) in acetonitrile (5 mL) was added to $[NEt_4]_3[Rh_7(CO)_{16}]$ (0.150 g, 0.0963 mmol) dissolved in 20 mL of acetonitrile. After 6 days, the mother solution was dried under vacuum and washed with ethanol (2 × 10 mL), THF (2 × 10 mL), and methanol (2 × 10 mL). Extraction in MeCN (20 mL) of the residue gave a mixture of $[HRh_{14}(CO)_{25}]^{3-}$ and $[Rh_{14}(CO)_{25}]^{4-}$. By the slow addition of a diluted solution of H_2SO_4 in acetonitrile, monitored via IR spectroscopy, $[Rh_{14}(CO)_{25}]^{4-}$ was successfully converted into $[HRh_{14}(CO)_{25}]^{3-}$. Crystals of $[NEt_4]_3[HRh_{14}(CO)_{25}]$ suitable for X-ray analysis were obtained by slow diffusion of hexane (1 mL) and diisopropyl ether (15 mL) onto the acetonitrile solution. The salt is soluble in acetone, acetonitrile, DMF, and dimethyl sulfoxide (DMSO) and insoluble in nonpolar solvents. Elem anal. Calcd for $[NEt_4]_3[HRh_{14}(CO)_{25}]$: C, 23.21; H, 2.41; N, 1.66; Rh, 56.93. Found: C, 23.5; H, 2.20; N, 1.81; Rh, 57.05.

Synthesis of $[Rh_{15}(CO)_{27}]^{3-}$ from $[Rh_7(CO)_{16}]^{3-}$ and $InCl_3\cdot xH_2O$. A suspension of $InCl_3\cdot xH_2O$ (0.030 g, 0.135 mmol) in acetonitrile (10 mL) was added to $[NEt_4]_3[Rh_7(CO)_{16}]$ (0.210 g, 0.135 mmol) dissolved in 20 mL of acetonitrile. After about 3 days, the mother solution was filtered, dried under vacuum, and washed with water (3 × 10 mL) and ethanol (2 × 10 mL). The extractions in THF (20 mL) and methanol (20 mL) gave very diluted solutions of other carbonyl species; the extraction in acetone (20 mL) was layered with hexane (15 mL), and after slow diffusion, it gave dark crystals of $[NEt_4]_3[Rh_{15}(CO)_{27}]$. The salt is soluble in acetonitrile, DMF, and DMSO and insoluble in nonpolar solvents. Elem anal. Calcd for $[NEt_4]_3[Rh_{15}(CO)_{27}]$: C, 22.8; H, 2.25; N, 1.56; Rh, 57.38. Found: C, 23.0; H, 2.38; N, 1.62; Rh, 57.95.

Synthesis of $[Rh_{15}(CO)_{25}(MeCN)_2]^{3-}$ from $[Rh_{15}(CO)_{27}]^{3-}$. A total of 70.1 mg of $[NEt_4]_3[Rh_{15}(CO)_{27}]$ was dissolved in acetonitrile, and the solution was layered with hexane and diisopropyl ether. After slow diffusion, black crystals of $[NEt_4]_3[Rh_{15}(CO)_{25}(MeCN)_2]\cdot 2MeCN$ suitable for X-ray analysis were obtained.

The salt is soluble in acetonitrile, DMF, and DMSO and insoluble in nonpolar solvents.

Synthesis of $[Rh_{17}(CO)_{37}]^{3-}$ from $[Rh_7(CO)_{16}]^{3-}$ and $ZnCl_2\cdot xH_2O$. A suspension of $ZnCl_2\cdot xH_2O$ (0.014 g, 0.102 mmol) in

(54) Longoni, G.; Femoni, C.; Iapalucci, M. C.; Zanello, P. *Metal Clusters in Chemistry*; Braunstein, P., Oro, L., Raithby, P., Eds.; VCH: Weinheim, Germany, 1999; Vol. II, pp 1137−1158.

(55) Allevi, C.; Heaton, B. T.; Seregni, C.; Strona, L.; Goodfellow, R. J.; Chini, P.; Martinengo, S. *J. Chem. Soc., Dalton Trans*. **1986**, 1375−1382.

(56) Keller, E. *SCHAKAL99*; University of Freiburg: Freiburg, Germany, 1999.

Table 6. Crystal Data for $[NEt_4]_3[Rh_{15}(CO)_{27}]$, $[NEt_4]_3[Rh_{15}(CO)_{25}(MeCN)_2]\cdot 2MeCN$, and $[NEt_4]_3[Rh_{17}(CO)_{37}]$

compound	$[NEt_4]_3[Rh_{15}(CO)_{27}]$	$[NEt_4]_3[Rh_{15}(CO)_{25}(MeCN)_2]\cdot 2MeCN$	$[NEt_4]_3[Rh_{17}(CO)_{37}]$
formula	$C_{51}H_{60}N_3O_{27}Rh_{15}$	$C_{57}H_{72}N_7O_{25}Rh_{15}$	$C_{61}H_{60}N_3O_{37}Rh_{17}$
fw	2690.67	2798.87	3176.59
T, K	298(2) K	293(2)	298(2)
λ, Å	0.71073	0.71073	0.71073
cryst syst	triclinic	monoclinic	monoclinic
space group	$P\bar{1}$	$P2(1)/n$	Cc
a, Å	16.867(2)	13.943(2)	24.4555(15)
b, Å	18.898(3)	28.788(5)	13.8637(15)
c, Å	23.275(3)	19.538(3)	26.961(3)
α, deg	88.282(2)	90	90
β, deg	88.360(2)	91.510(4)	109.257(2)
γ, deg	88.004(2)	90	90
cell vol., Å^3	7408.4(18)	7840(2)	8629.7(14)
Z	4	4	4
D_c, g cm^{-3}	2.412	2.371	2.445
μ, mm^{-1}	3.316	3.138	3.237
F(000)	5112	5352	6032
cryst size, mm	0.15 × 0.10 × 0.08	0.18 × 0.15 × 0.10	0.18 × 0.14 × 0.10
θ limits, deg	1.08−25.00	1.26−25.00	1.60−25.00
index ranges	$-20 \le h \le 20$, $-22 \le k \le 22$, $-27 \le l \le 27$	$16 \le h \le 16$, $-34 \le k \le 34$, $-23 \le l \le 23$	$-29 \le h \le 28$, $-15 \le k \le 16$, $-32 \le l \le 15$
reflns collected	70 757	68 919	14 688
indep reflns	26008 [R(int) = 0.0490]	13793 [R(int) = 0.1099]	8912 [R(int) = 0.0840]
completeness to θ = 25.00°, %	99.6	100.0	99.9
data/restraints/param	26 008/673/1766	13 793/202/941	8912/900/1063
GOF on F^2	1.031	1.098	1.136
R1 [$I > 2\sigma(I)$]	0.0691	0.0825	0.1083
wR2 (all data)	0.2215	0.2021	0.2491
largest diff. peak and hole, e Å^{-3}	2.523 and −1.452	4.062 and −1.724	1.791 and −2.228

acetone (10 mL) was added to $[NEt_4]_3[Rh_7(CO)_{16}]$ (0.320 g, 0.205 mmol) dissolved in 20 mL of acetone. After about 4−5 h, the mother solution was dried under vacuum and then washed with water (3 × 10 mL) and ethanol (2 × 10 mL). The extraction in methanol (20 mL) gave $[NEt_4]_3[Rh_{17}(CO)_{37}]$. Crystals suitable for X-ray analysis were obtained by drying of the above solution under vacuum, dissolution of the residue in acetone (15 mL) and layering of the new solution with hexane (1 mL) and diisopropyl ether (10 mL). The salt is soluble in acetone, acetonitrile, DMF, and DMSO and insoluble in nonpolar solvents. Elem anal. Calcd for $[NEt_4]_3[Rh_{17}(CO)_{37}]$: C, 23.04; H, 1.89; N, 1.32; Rh, 55.11. Found: C, 23.20; H, 2.10; N, 1.54; Rh, 55.40.

Synthesis of $[Rh_{17}(CO)_{30}]^{3-}$ from $[Rh_7(CO)_{16}]^{3-}$ and H_2SO_4. A solution of H_2SO_4 in acetonitrile was slowly added to $[NEt_4]_3[Rh_7(CO)_{16}]$ (1.28 g, 0.82 mmol) dissolved in 20 mL of acetonitrile in a 1.5:1 molar ratio. After about 4−5 h, the mother solution was dried under vacuum and washed with water (2 × 10 mL). The residue was extracted in THF (20 mL), and the solution was layered with hexane (15 mL). After slow diffusion of hexane into the THF solution, black crystals of $[NEt_4]_3[Rh_{17}(CO)_{30}]$ were obtained. The salt is well soluble in acetone, acetonitrile, DMF, and DMSO and insoluble in nonpolar solvents. Elem anal. Calcd for $[NEt_4]_3[Rh_{17}(CO)_{30}]$: C, 21.74; H, 2.01; N, 1.41; Rh, 58.74. Found: C, 21.90; H, 1.90; N, 1.55; Rh, 58.24.

X-ray Data Collection and Crystal Structure Determination of $[NEt_4]_3[Rh_{15}(CO)_{27}]$, $[NEt_4]_3[Rh_{15}(CO)_{25}(MeCN)_2]\cdot 2MeCN$, and $[NEt_4]_3[Rh_{17}(CO)_{37}]$. Crystal data and details of the data collection and refinement are given in Table 6. The diffraction experiments were carried out at room temperature on a Bruker APEXII diffractometer equipped with a CCD detector. Intensity data were corrected for Lorentz and polarization effects. An empirical absorption correction was applied by using *SADABS*.[57] The structure was solved by direct methods and refined by full-matrix least squares on F^2 using *SHELX97*.[58] H atoms were added in calculated positions (d_{C-H} = 0.93 Å), and their positions were not refined but continuously updated with respect to their C atoms and were given fixed isotropic thermal parameters.

Acknowledgment. We acknowledge the financial support of the Universities of Bologna and Siena and PRIN2006.

Supporting Information Available: X-ray crystallographic data files in CIF format and tables of bonding contacts for several trianions. This material is available free of charge via the Internet at http://pubs.acs.org.

IC0623718

(57) Sheldrick, G. M. *SADABS*; University of Göttingen: Göttingen, Germany, 1996.
(58) Sheldrick, G. M. *SHELX97*; University of Göttingen: Göttingen, Germany, 1997.